Near-field optical study of selective photomodification of fractal aggregates

W. David Bragg, Vadim A. Markel,* Won-Tae Kim, Katyayani Banerjee, Marvin R. Young,† Jane G. Zhu, Robert L. Armstrong, Vladimir M. Shalaev, and Z. Charles Ying‡

Department of Physics, New Mexico State University, Las Cruces, New Mexico 88003

Yulia E. Danilova and Vladimir P. Safonov

Institute of Automation and Electrometry, Novosibirsk, 630090, Russia

Received July 12, 2000; revised manuscript received November 30, 2000

Selective photomodification of fractal aggregates of silver nanoparticles is studied experimentally by photon-scanning-tunneling microscopy. Near-field optical images of the aggregates before and after photomodification show changes in the distribution of local electromagnetic fields in the near zone at subwavelength scale. These changes are much stronger than those measured in the far field. Results from numerical modeling of photomodification are in qualitative agreement with the experimental observations. © 2001 Optical Society of America

OCIS codes: 310.6860, 180.5810, 260.2110.

1. INTRODUCTION

Near-field optical properties of rough nanometer-structured metallic surfaces (RNSMS's) with fractal geometry have been a subject of intensive investigation in the past several years.[1–10] The possibility of employing RNSMS's for single-molecular spectroscopy[5–7] and for giant enhancement of local nonlinear responses,[10–12] among other exciting effects, has been discussed in the literature. In this paper we report the first near-field experimental observation of changes in the local electromagnetic field owing to the effect of selective photomodification[13] of RNSMS's. Previous far-field optical studies have shown photomodification of three-dimensional fractals, manifested by appearance of spectral- and polarization-dependent holes in the absorption spectra.[14–16] These spectral holes are associated with local restructuring of the fractal aggregates, as revealed in parallel studies of optical spectrum and electron microscopy.[16] In this paper we investigate the changes in the local electromagnetic fields excited near RNSMS's by a weak probe beam after irradiation by a stronger photomodifying laser pulse. These changes are observed in the near field with the use of photon-scanning-tunneling microscopy (PSTM).

It is well established that a combination of electromagnetic interaction and the fractal geometry leads to a strong enhancement of local electromagnetic fields near RNSMS's in a spectral range that is much wider than the absorption band of individual metal nanoparticles. It turns out that for any wavelength from ~ 0.5 μm to at least ~ 10 μm, the fractal RNSMS's possess a number of collective resonant modes (plasmon modes). Typically, for each frequency, some of the resonant modes are localized and some are delocalized, a behavior referred to as inhomogeneous localization.[17–19] There exist areas of nanometer dimensions in the distribution of local electromagnetic fields near RNSMS's (called hot spots), where the local electric field exceeds the applied field by several orders of magnitude.[11,12,20–23] The presence of hot spots in RNSMS's has been observed directly with near-field optical microscopy.[1,4,8]

When the intensity of the electric field in a hot spot exceeds some threshold value, irreversible changes in the geometrical structure occur. Therefore irradiation of silver fractal aggregates by a laser pulse with energy above a threshold leads to photoburning of a spectral hole in the absorption spectrum of the aggregates near the irradiation laser wavelength.[13,14,16,24] It was shown that the aggregate structure as a whole remains the same after irradiation, but particles within some nanometer-scale regions change their shape and local arrangement.[16] The electron-microscopic study suggests that the sizes of hot spots in the fractal material are $\leqslant 100$ nm and decrease as the photomodification laser wavelength increases,[16] which is in qualitative agreement with theoretical predictions.[4,8,10,20,21,23]

After photomodification with laser energy near the threshold, the absorption coefficient of the whole sample changes only by $\sim 1\%$.[16] However, the question of whether this small change in the optical response is evenly distributed in space over the whole sample or highly localized in certain areas remains open. While it is known that the geometrical restructuring that results from photomodification is confined to small areas,[16] it is not clear if the same is true for the changes in local electromagnetic fields in the near-field zone. In this paper we investigate experimentally and numerically the sizes and locations of the areas where the local electromagnetic fields are changed by the photomodification. The experiments were carried out with photon-scanning-tunneling

0740-3224/2001/050698-08$15.00

microscopy (PSTM), which is a form of near-field optical microscopy, and with atomic-force microscopy (AFM). We show that the changes in the local electromagnetic field observed in the near zone owing to photomodification significantly exceed the change in the far field that can be registered, for example, in absorption measurements.

The paper is organized as follows. In Section 2 we describe our experimental setup and procedures. Sections 3 and 4 contain the discussion of our experimental and numerical simulation results, respectively. Finally, Section 5 summarizes the results.

2. EXPERIMENTAL PROCEDURE

The fractal samples used in our experiments were synthesized by two different methods. In the first method, fractal aggregates of silver nanoparticles of ~20 nm in diameter were grown in a colloidal solution prepared from silver nitrate and sodium citrate[25] and deposited onto a glass substrate. This type of silver colloidal aggregates has been characterized with electron microscopy and used in our previous far-field optical research.[16,26] Fractal aggregates were also prepared by laser ablation of a silver target placed in a vacuum chamber backfilled with a buffer gas.[24] A Nd:YAG laser (Quanta-Ray DCR) that provided 8-ns, 1064-nm pulses at a 10-Hz repetition rate was used as the light source. Silver nanoparticles were formed during laser ablation and then aggregated into fractal clusters in a buffer gas during the diffusion-limited aggregation process.[24] The fractal clusters eventually settled down on a glass substrate placed at the bottom of the chamber, forming a thin film of fractal RNSMS's. Our electron-microscopic study showed that a fractal cluster of this type consists of hundreds to thousands of nanoparticles.

The fractal samples prepared by both methods were studied with a photon-scanning tunneling microscope, which was modified from a commercial atomic-force microscope (Quesant Q250). Samples were mounted onto the hypotenuse face of a right-angle prism with index-matching fluid and illuminated by the evanescent field in the total-internal-reflection geometry. The illumination source was a helium–neon laser at a wavelength of either 543 or 633 nm. In the spectroscopic study a tunable diode laser (Newport 2010) was used. The local optical signal was collected through an uncoated optical fiber,[27] which was sharpened to approximately 50 nm in radius at the tip end by a fiber puller (Sutter Instruments P-2000). The separation between the fiber tip and a sample was regulated with nonoptical shear-force feedback.[28] The photomodification was achieved by irradiating the sample *in situ* from above, with 5-ns pulses of the second-harmonic output of a Nd:YAG laser (Quantel Brilliant) at 532 nm.

The geometrical properties of the fractal samples were studied with transmission-electron microscopy (TEM). Two microscopes (Hitachi H-7000 and JEM-100CX) were used in the experiments.

3. EXPERIMENTAL RESULTS

Figure 1(a) shows a near-field optical image of silver colloidal aggregates. The illumination source during the PSTM scan was a He–Ne laser at 543 nm and was *s* polarized. The image shows a nonuniform distribution of optical intensity, as predicted theoretically[23,29–31] and observed in previous experiments.[1,4,8] The minimum feature size is ~200 nm, corresponding to the lateral resolution of our microscope. The theoretically predicted minimum feature size is smaller by an order of magnitude.[23] The magnitude of the observed intensity fluctuations is smaller than what the theories predict, probably because of the limited resolution of the microscope.

Figure 2 exhibits 12 near-field optical images recorded at the same 10 μm × 10 μm area of a sample with different probing wavelengths from 760 to 820 nm. All those images exhibit hot spots. The images with small wavelength differences (~10 nm) appear correlated. The correlation decreases as the wavelength difference increases. These results are consistent with a recent study.[8]

Photomodification experiments were carried out in the following way: First, a set of PSTM and AFM images was recorded simultaneously. The scan was repeated a few times to demonstrate stability of the images. Figure 1(a) shows one of such PSTM images. (The corresponding AFM image used to register the location of the imaged area is not shown.) The tip was then retracted, and the sample was irradiated with ten *s*-polarized, 532-nm, 5-ns pulses from the Nd:YAG laser, incident upon the sample at an angle of 70° with respect to the surface normal. The retraction of the tip avoided possible damage to the tip by the nanosecond pulses and possible perturbation of the optical field by the tip. Finally, another set of PSTM and AFM images was recorded.

Figure 1(b) shows the PSTM image after irradiation, which exhibits significant differences from the image before irradiation [Fig. 1(a)]. The intensity profiles of the optical images along the marked line ($y = 3.0\ \mu$m) are also plotted in Fig. 1. Two hot spots present before irradiation, marked by arrows, decrease their intensities by a

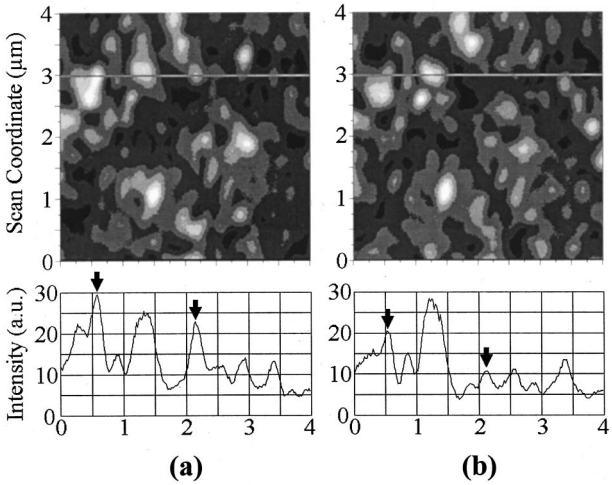

Fig. 1. PSTM images of a silver fractal film (a) before and (b) after photomodification of the sample with nanosecond laser pulses at 532 nm. The images were recorded with a probe (imaging) beam wavelength at 543 nm. Optical intensity profiles along the marked curves are also shown.

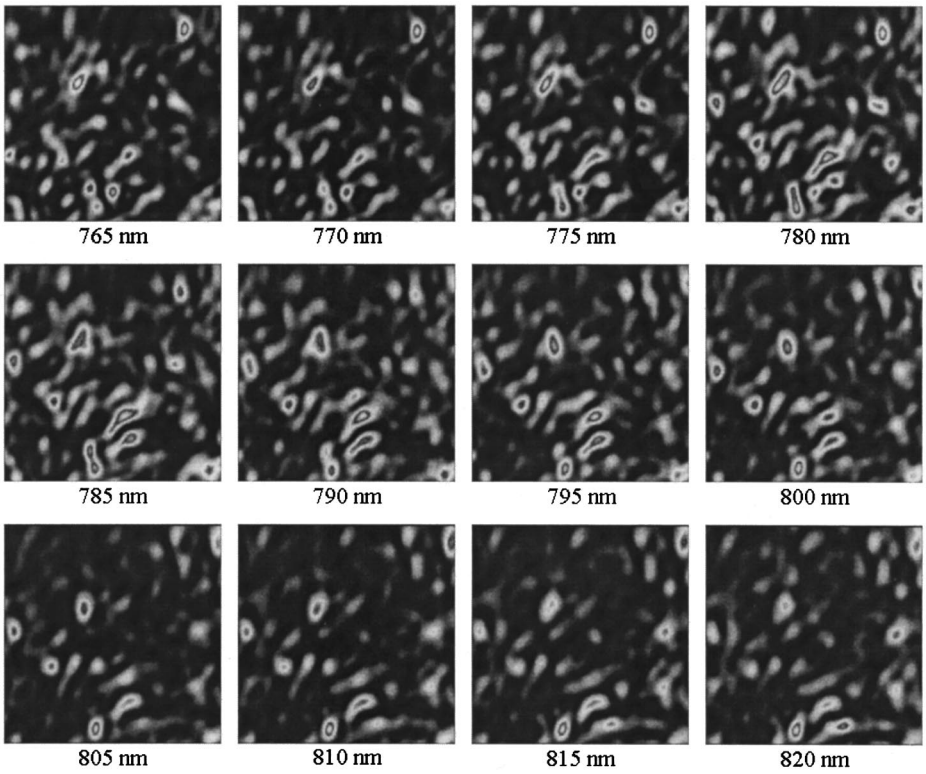

Fig. 2. PSTM images of a silver fractal film recorded at various probe-beam wavelengths from 765 to 820 nm. Each image is 10 μm $\times$ 10 μm in size.

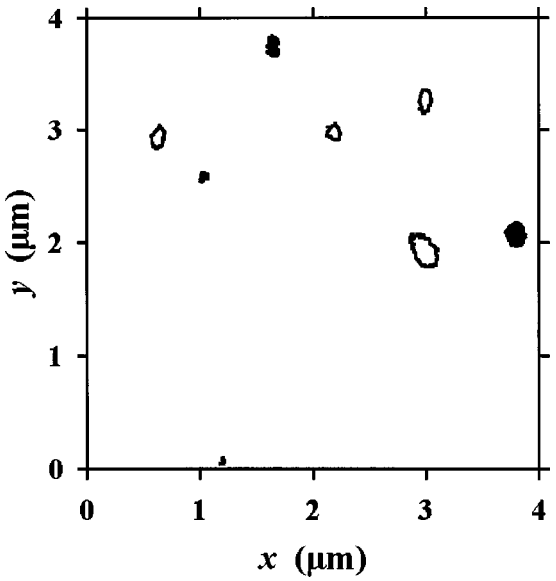

Fig. 3. Difference in optical intensity of the two images of Fig. 1. The new hot spots are highlighted in black. The diminished hot spots are indicated by open contours.

factor of ~2 after the irradiation. The magnitudes of these local changes are much greater than the ~1% change in the absorption coefficient of the sample measured in the far field.[16] The photomodifying irradiation also creates new hot spots. One such new hot spot, for example, is created after the irradiation at $x = 3.8\,\mu$m and $y = 2.1\,\mu$m.

We have computed the irradiation-induced change in optical intensity at each pixel in the whole image area. The result is plotted in Fig. 3. In order to highlight large changes, only areas where the intensity change exceeds 3σ, where σ is the average value of the local intensity changes over the whole scanning area of 4 μm $\times$ 4 μm, are plotted. There are four areas, indicated in black, where the local optical intensity increases by at least 3σ after irradiation. The new hot spot at $x = 3.8\,\mu$m and $y = 2.1\,\mu$m, as mentioned earlier, is one of them. There are also four areas, circled by open contours, where the original hot spots diminish substantially after irradiation. Two of them are located at $y = 3.0\,\mu$m, where the optical intensity profiles are shown in Fig. 1. Note that the areas where the local optical intensity changes substantially are distributed sparsely in Fig. 3; the photomodification occurs mainly in a few areas of nanometer dimensions.

When a fractal RNSMS is irradiated at 532 nm, resonant modes with wavelengths around 532 nm are excited, and nanoparticles in the corresponding hot spots are restructured. This leads to observation of the photomodification at a probe wavelength of 543 nm since this value is close to 532 nm. Because the restructured nanoparticles also participate in the excitation of other resonant modes at various wavelengths, photomodification may also occur when probed at wavelengths far from 532 nm. Figure 4 shows PSTM images obtained with a probe beam at 633 nm, before and after irradiation. Significant photomodification was observed even though 633 nm is at the long-wavelength edge of a spectral hole burned by laser pulses at 532 nm. A hot spot at $x = 0.5\,\mu$m and $y = 0.9\,\mu$m diminishes its intensity after irradiation, and a new hot spot at $x = 2.3\,\mu$m and $y = 0.0\,\mu$m is created.

The photomodification process exhibits a threshold nature. While photomodification was seen after irradiation at 9.5 mJ/cm^2 (see Fig. 1), no significant changes were observed in PSTM images after irradiation at intensities of 8.5 mJ/cm^2 or lower. These observations indicate a threshold energy density of approximately 9 mJ/cm^2, which is in general agreement with a previous study, where a threshold of 12 mJ/cm^2 was reported from measurements of spectral holes in the far-field optical absorption.[16] These values of threshold are very low. If a nanosecond laser pulse is incident upon a piece of bulk silver at an incident energy density of 9 mJ/cm^2, the temperature rise is calculated[32] to be ~1 K.

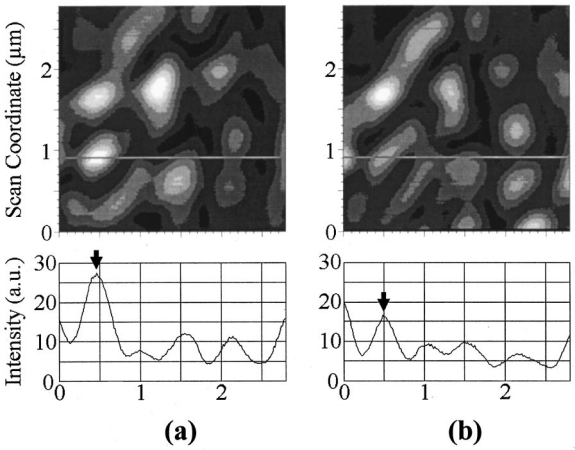

Fig. 4. Same as Fig. 1, except that a different sample area is imaged with a probe-beam wavelength at 633 nm.

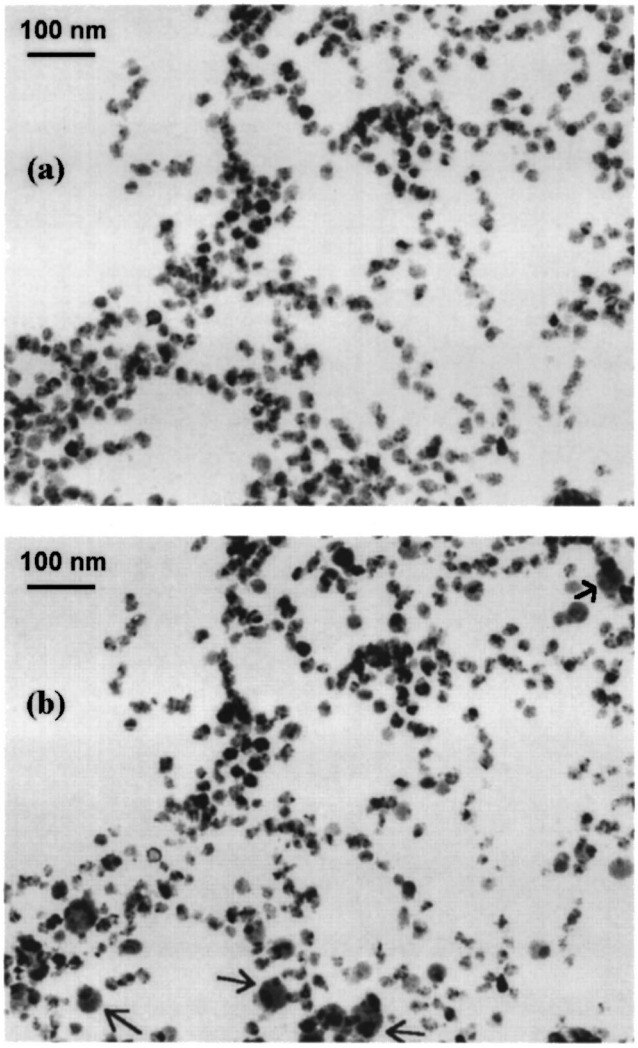

Fig. 5. TEM images of aggregated silver nanoparticles (a) before and (b) after irradiation of nanosecond laser pulses at a wavelength of 1079 nm. The incident energy density was 11 mJ/cm^2 per pulse.

Experiments on fractal samples prepared by the laser ablation technique showed similar results. The threshold energy density is approximately 8 mJ/cm^2 for photomodification of the laser-ablated samples.

The nature of the photomodification was revealed by TEM studies. Figure 5(a) shows a TEM image of a fractal sample, which consists of aggregated silver nanoparticles with an average diameter of 22 nm. After recording this microscopic image, the sample was removed from the electron microscope and irradiated with 10-ns laser pulses at a wavelength of 1079 nm. The incident energy density was 11 mJ/cm^2 per pulse. After laser irradiation, the sample was reinserted into the electron microscope and another image was recorded at the same area of Fig. 5(a). The TEM image after the irradiation, shown in Fig. 5(b), exhibits many features identical to those in Fig. 5(a). The overall arrangement of the nanoparticles in these two images, as well as locations and shapes of most of the individual nanoparticles, is the same. There are, however, locations (indicated by arrows) where several nanoparticles appear sintered after laser irradiation. It is suggested that these are the locations of the hot spots, where the local heating leads to the sintering of the nanoparticles. The sizes of these sintering regions are of the order of ~50 nm, consistent with the theoretical predictions of hot-spot sizes much smaller than the irradiation wavelength.

The local temperatures at hot spots are estimated to be below the melting temperature of silver for an irradiation laser energy just above the threshold.[16] Karpov, Popov, and Slabko have observed recently photostimulated fractal aggregation of colloidal silver particles using a cw light source at low light intensities (of the order of 1 mW/cm^2) and attribute it to the two-photon photoelectric effect.[33] Zhu and Averback have demonstrated by molecular dynamic simulations that metal nanoparticles that are in contact with each other and heated evenly to only ~1/2 of the melting temperature may not behave as rigid bodies.[34] In particular, the local shear stress near the necks (touching points) was shown to be large enough to cause plastic deformation and eventual sintering of the nanoparticles in a 100-ps time scale. There is experimental evidence to support their conclusion.[35] Although the exact mechanism of the photomodification is not completely understood at the present time, it seems very plausible that photomodification is caused by such sintering.

Figure 6 shows TEM images of another fractal sample (a) before and (b) after laser irradiation. Here a laser wavelength of 450 nm, an incident energy density of 20 mJ/cm^2 per pulse, and a total of ten pulses were used. The image recorded after the laser irradiation, Fig. 6(b), exhibits a number of sintered particles. This result is

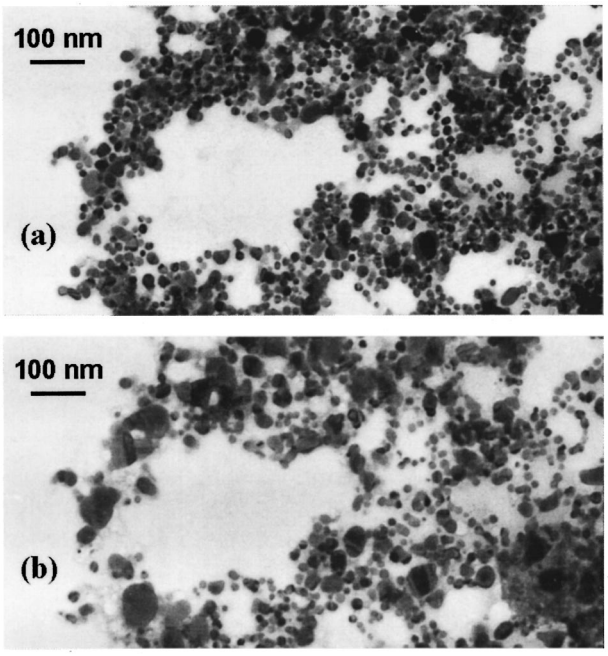

Fig. 6. TEM images of aggregated silver nanoparticles (a) before and (b) after irradiation of nanosecond laser pulses at a wavelength of 450 nm. The incident energy density was 20 mJ/cm^2 per pulse.

qualitatively similar to those shown in Fig. 5. There are many more sintered particles, however, in the latter case.

The extent of sintering and photomodification depends on both laser pulse energy and laser wavelength. As discussed earlier, there is a threshold energy for photomodification. No photomodification, limited photomodification, or extensive photomodification occurs below the threshold, just above the threshold or well above the threshold, respectively. The threshold varies with laser wavelength owing to changes in the quality factor of the plasmon mode and perhaps the reflectivity of the light. A higher-quality factor provides a sharper hot spot with higher local enhancement and therefore a higher local temperature. The quality factor increases as wavelength increases for silver in the visible and near infrared.

4. NUMERICAL SIMULATION RESULTS

To gain further insight, we modeled the photomodification process and carried out numerical simulation of the photomodification of near-field optical intensity. In our simulations, we assume that nanoparticles that are exposed to an optical intensity higher than a threshold value are removed from the sample and do not contribute to the optical absorption at a wavelength close to that of the modification laser beam. This method of numerical simulation of the photomodification of fractal clusters was first proposed in Ref. 13. It was presumed in that study that the local temperature becomes so high in the monomers exposed to high local-field intensity that they can melt and eventually evaporate. This amounts to removal of the material from the cluster and the appearance of narrow holes in the absorption spectrum (which were also shown to be polarization selective). Thus the integral of the absorption cross section over the wavelengths where absorption is not negligibly small is reduced by this process of spectral hole burning. The spectral- and polarization-selective holes in absorption spectra of fractal silver colloids were observed experimentally,[14,15] in agreement with the theoretical predictions.[13] The TEM results presented earlier suggest sintering rather than the loss (evaporation) of material. Sintering still results in the appearance of the holes in the absorption spectra but also in the increased absorption at wavelengths that are far from the modifying laser wavelength; thus the integral of absorption over the wavelengths is conserved. This phenomenon was observed experimentally[14,15] but is difficult to simulate precisely. It should be noted, however, that plasmon oscillations represent geometrical resonances. Frequencies of plasmon modes in a fractal depend on the local structures of the areas where the modes are localized. The photomodification leads to sintering (coalescence) of particles in these areas and thus a change of their local geometry. Therefore after the modification such areas do not resonate any more at the same frequency; thus their interaction with light can be neglected as an appropriate approximation. Since we are interested mainly in the local-field distributions at wavelengths that are close to the modifying wavelength, we adopt here the model of Ref. 13.

To simulate a fractal sample, we first generated a three-dimensional lattice cluster-cluster aggregate of 5000 particles according to the Meakin algorithm.[36,37] The fractal dimension of a generated aggregate was close to 1.8.[37] Then the aggregate was deposited onto a plane surface and allowed to undergo a vertical collapse: the particles that had an empty space directly beneath them were allowed to fall until they hit the surface plane or another particle underneath. As a result, there were no empty spaces underneath particles. Naturally, this projection of a three-dimensional object to a quasi-two-dimensional structure resulted in a drastic restructuring. The height–height correlation function of an ensemble of such quasi-two-dimensional aggregates was shown to have a large scaling region with a slope corresponding to the fractal dimension $D = 2.6$.[4] This observation leads to the conclusion that the original self-similar fractals became self-affine structures after deposition on a plane, having different scaling properties in the (x, y) plane and in the normal, z direction. The computer-simulated structures provide a good resemblance of the electron-microscopy images of the aggregates deposited onto a glass substrate (see the images in Ref. 4).

In our model we used a refractive index of 1.52 for the prism. The photomodification beam at the wavelength of 532 nm is incident at an angle of 70°, in accordance with the experimental setup. We took into account the reflected beam, with the reflection coefficient calculated according to the Fresnel formulas. The probe beam underwent a total internal reflection from the inner surface of the prism so that the evanescent field excited the sample, as in the experimental setup:

$$\mathbf{E}_{ev}(\mathbf{r}) = \mathbf{E}_0 \exp\left[\frac{\omega}{c}(-z\sqrt{n^2 \sin^2\theta - 1} + ixn \sin\theta)\right], \quad (1)$$

where the x axis coincides with the longitudinal direction of the evanescent field propagation, the z axis is normal to the prism surface, and the θ is the angle of incidence with respect to the z axis. The total-internal-reflection condition, $n \sin \theta > 1$, is met for $\theta = 45°$ and $n = 1.52$.

The local field at the sample was calculated with the coupled-dipole equations (CDE's). These equations were introduced originally[38] in the context of the discrete dipole approximation[39,40] and later for calculating the optical properties of fractal clusters of small spherical monomers[13,21] and molecular aggregates.[41] According to Refs. 13 and 21, each spherical monomer is represented by an oscillating dipole that can interact with the incident wave and other dipoles by dipole radiation fields. The CDE method does not take into account higher multipole moments of monomers, which were shown to be important for interaction of nearest-neighbor monomers.[42,43] In particular the CDE in its pure form underestimates the interaction strength of nearest-neighbor monomers and, as a result, predicts much-smaller spectral shifts of resonance lines than were observed experimentally,[43] and, in particular, in silver fractal colloids.[44,45] A method of renormalization of fractal clusters was proposed[26,46] that allows one to overcome this difficulty and to stay within the dipole approximation, without the tremendous numerical complication of considering all higher multipoles. It should be also noted that the numerical methods that take into account higher multipoles[47,48] demonstrate very slow convergence of results (with an increase of the maximum multipole number) for materials with metal-type dielectric functions, which exhibit strong optical resonances. The renormalization method introduces geometrical intersection of nearest-neighbor monomers and keeps simultaneously the total size, volume, and two-point density–density correlation functions of a cluster unchanged. This is achieved by simultaneously changing the number of monomers in the cluster, N, the monomer radius, a, and the distance between two neighboring monomers, l, from their experimental values to certain renormalized values (see the renormalization formulas in Ref. 46).

The CDE's have the form

$$\mathbf{d}_i = \alpha\left[\mathbf{E}_{\mathrm{ev}}(\mathbf{r}_i) + \sum_{j\neq i} G(\mathbf{r}_i - \mathbf{r}_i)\mathbf{d}_j\right]. \tag{2}$$

Here $\alpha = a^3(\epsilon - 1)/(\epsilon + 1)$ is the polarizability of a monomer, where ϵ is the complex dielectric constant for silver taken from the experimental data,[49] $\hat{G}(\mathbf{r})$ is the regular part of the free space (dyadic) Green's function for the vector wave equation, and $\mathbf{r}_i$ and $\mathbf{d}_i$ are the location and dipole moment of the ith monomer. The solution of the above equations allows one to find the electric field anywhere in space according to

$$\mathbf{E}(\mathbf{R}) = \sum_{i=1}^{N} \hat{G}(\mathbf{R} - \mathbf{r}_i)\mathbf{d}_i + \mathbf{E}_{\mathrm{ev}}(\mathbf{R}). \tag{3}$$

The renormalization procedure is manifested in the value of the monomer radius a that enters the definition of α: it is taken to be larger than 1/2 of the distance l between the centers of two nearest-neighbor monomers (the lattice unit). According to Ref. 26, we selected α from the condition $l^3 = 4\pi a^3/3$.

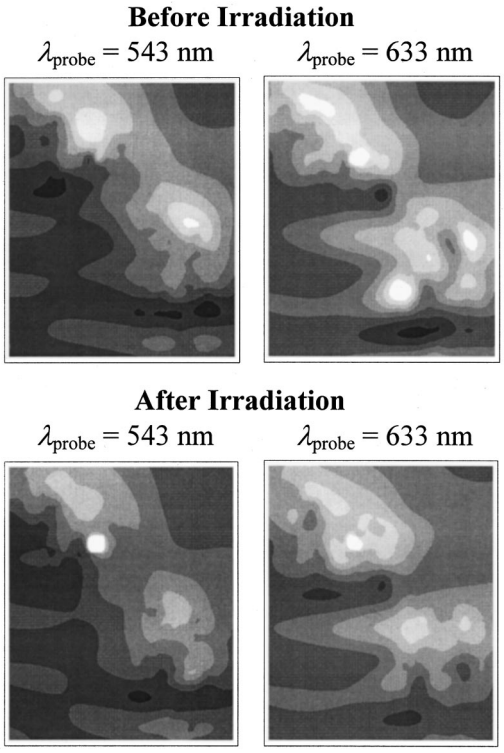

Fig. 7. Simulated near-field optical images at 543 and 633 nm of a computer-generated fractal silver aggregate deposited on a surface before and after photomodification. The dimensions of each image are 0.9 μm × 1.15 μm. The difference in optical intensity between two adjacent gray scales is 10%.

In our calculations we assumed that the tip does not perturb significantly the surface field distribution; this assumption is reasonable since the polarizability of resonant metal particles is much higher than that of the uncoated tip. After calculating the local electric field, we removed 500 particles (10%) that were exposed to the most-intense field. Local optical intensity was calculated before and after the photomodification with two probe wavelengths, 543 and 633 nm. The effect of finite resolution of the microscope was taken into account in the simulation by averaging the theoretical result over a finite area. The simulated images are shown in Fig. 7. The simulations show that photomodification occurs mainly in the vicinity close to the original hot spots. Local responses in many hot spots decrease after the photomodification. At the same time, some new hot spots are created, which can be traced to changes in the fractal structure by the photomodification. Spectroscopically, local photomodification leads to spectral holes close to the photomodification wavelength. These findings are in agreement with experimental results reported in this paper and earlier.[16]

5. SUMMARY

The following picture for the photomodification process emerges from our experimental and theoretical studies: During nanosecond-laser irradiation of a fractal sample, the laser energy is not uniformly distributed over the

sample surface. Rather, it is localized in hot spots owing to fractal geometry and electromagnetic interaction in rough nanometer-structured metallic surfaces (RNSMS's). Nanoparticles within some hot spots of nanometer dimensions are restructured if the incident laser energy exceeds a threshold of ~ 9 mJ/cm^2 per pulse. Such geometric changes in turn result in modification of local optical intensity. Some previously existing hot spots are diminished after irradiation, and new hot spots are created when probed at wavelengths either close to or far away from the irradiation laser wavelength. These local optical changes occur at locations that are determined by the local geometry of samples and differ from sample to sample. (We note that the field distributions are chaotically deterministic, i.e., they are random but reproducible.) The local contrast changes (by factors of ~ 2) are much greater than the spectral hole in the absorption coefficient measured in the far field ($\sim 1\%$).

ACKNOWLEDGMENTS

This research was supported in part by the National Science Foundation under grants DMR-9810183 and DMR-0071901, the U.S. Army Research Office under grant DAAG55-98-1-0425, NASA under grant NAG8-1710, the Petroleum Research Fund under grant 35028-AC5, the National Center for Supercomputing Application under grant PHY980006N, New Mexico Universities Collaborative Research of Los Alamos National Laboratory, and the Russian Foundation for Basic Research under grant 99-02-16670.

*Present address: Department of Electrical Engineering, Washington University, St. Louis, Missouri 63130.

†Present address: Celion Networks, Inc., Richardson, Texas 75082.

‡The e-mail address of Z. C. Ying is zcying@nmsu.edu.

REFERENCES

1. D. P. Tsai, J. Kovacs, Z. Wang, M. Moskovits, V. M. Shalaev, J. S. Suh, and R. Botet, "Photon scanning-tunneling-microscopy images of optical-excitation of fractal metal colloid clusters," Phys. Rev. Lett. **72**, 4149–4152 (1994).
2. S. I. Bozhevolnyi, B. Vohnsen, A. V. Zayats, and I. I. Smolyaninov, "Fractal surface characterization: implications for plasmon polariton scattering," Surf. Sci. **356**, 268–274 (1996).
3. S. I. Bozhevolnyi, "Localization phenomena in elastic surface-polariton scattering caused by surface roughness," Phys. Rev. B **54**, 8177–8185 (1996).
4. S. I. Bozhevolnyi, V. A. Markel, V. Coello, W. Kim, and V. M. Shalaev, "Direct observation of localized dipolar excitations on rough nanostructured surfaces," Phys. Rev. B **58**, 11441–11448 (1998).
5. K. Kneipp, Y. Wang, H. Kneipp, L. T. Perelman, I. Itzkan, R. R. Dasari, and M. S. Feld, "Single molecule detection using surface-enhanced Raman scattering (SERS)," Phys. Rev. Lett. **78**, 1667–1670 (1997).
6. K. Kneipp, H. Kneipp, V. B. Kartha, R. Manoharan, G. Deinum, I. Itzkan, R. R. Dasari, and M. S. Feld, "Detection and identification of a single DNA base molecule using surface-enhanced Raman scattering (SERS)," Phys. Rev. E **57**, R6281–6284 (1998).
7. K. Kneipp, H. Kneipp, R. Manoharan, I. Itzkan, R. R. Dasari, and M. S. Feld, "Extremely large enhancement factors in surface-enhanced Raman scattering for molecules on colloidal gold clusters," Appl. Spectrosc. **52**, 1493–1497 (1998).
8. V. A. Markel, V. M. Shalaev, P. Zhang, W. Huynh, L. Tay, T. L. Haslett, and M. Moskovits, "Near-field optical spectroscopy of individual surface-plasmon modes in colloid clusters," Phys. Rev. B **59**, 10903–10909 (1999).
9. E. Y. Poliakov, V. M. Shalaev, V. Shubin, and V. A. Markel, "Enhancement of nonlinear processes near rough nanometer-structured surfaces obtained by deposition of fractal colloidal sliver aggregates on a plain substrate," Phys. Rev. B **60**, 10739–10742 (1999).
10. V. M. Shalaev, *Nonlinear Optics of Random Media: Fractal Composites and Metal Dielectric Films* (Springer-Verlag, Berlin, 2000).
11. E. Y. Poliakov, V. M. Shalaev, V. A. Markel, and R. Botet, "Enhanced Raman scattering from self-affine thin films," Opt. Lett. **21**, 1628–1630 (1996).
12. E. Y. Poliakov, V. A. Markel, V. M. Shalaev, and R. Botet, "Nonlinear optical phenomena on rough surfaces of metal thin films," Phys. Rev. B **57**, 14901–14913 (1998).
13. L. S. Markel, V. A. Muratov, and M. I. Stockman, "Optical properties of fractals: theory and numerical simulation," Sov. Phys. JETP **71**, 455–464 (1990).
14. A. V. Karpov, A. K. Popov, S. G. Rautian, V. P. Safonov, V. V. Slabko, V. M. Shalaev, and M. I. Shtokman, "Observation of a wavelength- and polarization-selective photomodification of silver clusters," JETP Lett. **48**, 571–575 (1988).
15. Y. E. Danilova, A. I. Plekhanov, and V. P. Safonov, "Experimental study of polarization-selective holes, burning in absorption spectra of metal fractal clusters," Physica A **185**, 61–65 (1992).
16. V. P. Safonov, V. M. Shalaev, V. Markel, Y. E. Danilova, N. N. Lepeshkin, W. Kim, S. G. Rautian, and R. L. Armstrong, "Spectral dependence of selective photomodification in fractal aggregates of colloidal particles," Phys. Rev. Lett. **80**, 1102–1107 (1998).
17. M. I. Stockman, L. N. Pandey, and T. F. George, "Inhomogeneous localization of polar eigenmodes in fractals," Phys. Rev. B **53**, 2183–2186 (1996).
18. M. I. Stockman, "Inhomogeneous eigenmode localization, chaos, and correlations in large disordered clusters," Phys. Rev. E **56**, 6494–6507 (1997).
19. M. I. Stockman, "Chaos and spatial correlations for dipolar eigenproblems," Phys. Rev. Lett. **79**, 4562–4565 (1997).
20. V. M. Shalaev and M. I. Stockman, "Optical properties of fractal clusters (susceptibility, surface enhanced Raman scattering by impurities)," Sov. Phys. JETP **65**, 287–294 (1987).
21. V. A. Markel, L. S. Muratov, M. I. Stockman, and T. F. George, "Theory and numerical simulation of optical properties of fractal clusters," Phys. Rev. B **43**, 8183–8195 (1991).
22. V. M. Shalaev, E. Y. Poliakov, and V. A. Markel, "Small-particle composites. 2. Nonlinear optical properties," Phys. Rev. B **53**, 2437–2449 (1996).
23. V. M. Shalaev, "Electromagnetic properties of small-particle composites," Phys. Rep. **272**, 61–137 (1996).
24. A. I. Plekhanov, G. L. Plotnikov, and V. P. Safonov, "Production and spectroscopic study of silver fractal clusters by laser vaporation of target," Opt. Spectrosc. (USSR) **71**, 451–454 (1991).
25. P. Lee and D. Meisel, "Adsorption and surface-enhanced Raman of dyes on silver and gold sols," J. Phys. Chem. **86**, 3391 (1982).
26. V. A. Markel, V. M. Shalaev, E. B. Stechel, W. Kim, and R. L. Armstrong, "Small-particle composites. 1. Linear optical properties," Phys. Rev. B **53**, 2425–2436 (1996).
27. S. I. Bozhevolnyi, B. Vohnsen, E. A. Bozhevolnaya, and S. Berntsen, "Self-consistent model for photon scanning tunneling microscopy: implications for image formation and light scattering near a phase-conjugating mirror," J. Opt. Soc. Am. A **13**, 2381–2392 (1996).
28. M. Lee, E. B. McDaniel, and J. W. P. Hsu, "An impedance based non-contact feedback control system for scanning

probe microscopes," Rev. Sci. Instrum. **67**, 1468–1471 (1996).
29. A. V. Butenko, V. M. Shalaev, and M. I. Stockman, "Giant impurity nonlinearities in optics of fractal clusters," Sov. Phys. JETP **67**, 60–69 (1988).
30. V. M. Shalaev, R. Botet, D. P. Tsai, J. Kovacs, and M. Moskovits, "Fractals: localization of dipole excitations and giant optical polarizabilities," Physica A **207**, 197–207 (1994).
31. M. I. Stockman, L. N. Pandey, L. S. Muratov, and T. F. George, "Giant fluctuations of local optical-fields in fractal clusters," Phys. Rev. Lett. **72**, 2486–2489 (1994).
32. J. F. Ready, *Effects of High-Power Laser Radiation* (Academic, New York, 1971).
33. S. V. Karpov, A. K. Popov, and V. V. Slabko, "Observation of the two-photon photoelectric effect in low-intensity optical fields during photostimulated fractal aggregation of colloidal silver," JETP Lett. **66**, 106–110 (1997).
34. H. Zhu and R. S. Averback, "Sintering processes of two nanoparticles: a study by molecular dynamics," Philos. Mag. Lett. **73**, 27–33 (1996).
35. S. E. Rorak, A. Lo, R. T. Skodje, and K. L. Rowlen, "Changes in thin-metal-film nanostructure at near-ambient temperatures," in *Nanostructured Materials: Clusters, Composites, and Thin Films*, V. M. Shalaev and M. Moskovits, eds. (American Chemical Society, Washington D.C., 1998), pp. 152–168.
36. P. Meakin, "Formation of fractal clusters and networks by irreversible diffusion-limited aggregation," Phys. Rev. Lett. **51**, 1119–1122 (1983).
37. V. A. Markel, V. M. Shalaev, E. Y. Poliakov, and T. F. George, "Numerical studies of second-and fourth-order correlation functions in cluster-cluster aggregates in application to optical scattering," Phys. Rev. E **55**, 7313–7333 (1997).
38. E. M. Purcell and C. R. Pennypacker, "Scattering and absorption of light by nonspherical dielectric grains," Astrophys. J. **186**, 705–714 (1973).
39. B. T. Draine, "The discrete-dipole approximation and its application to interstellar graphite grains," Astrophys. J. **333**, 848–872 (1988).
40. B. Draine and P. Flatau, "Discrete-dipole approximation for scattering calculations," J. Opt. Soc. Am. A **11**, 1491–1499 (1994).
41. D. Keller and C. Bustmante, "Theory of the interaction of light with large inhomogeneous molecular aggregates. II. Psi-type circular dichroism," J. Chem. Phys. **84**, 2972–2980 (1986).
42. J. E. Sansonetti and J. K. Furdyna, "Depolarization effects in arrays of spheres," Phys. Rev. B **22**, 2866–2874 (1980).
43. F. Claro, "Absorption spectrum of neighbouring dielectric grains," Phys. Rev. B **25**, 7875–7876 (1982).
44. Y. E. Danilova, S. V. Karpov, A. K. Popov, S. G. Rautian, V. P. Safonov, V. V. Slabko, V. M. Shalaev, and M. I. Stockman, "Experimental investigation of optical nonlinearities of silver fractal clusters," in *Proceedings of the X International Vavilov Conference on Nonlinear Optics*, S. G. Rautian, ed. (Nova Science, New York, 1992), pp. 295–302.
45. Y. E. Danilova, V. A. Markel, and V. P. Safonov, "Light absorption by random clusters of silver particles," Atmos. Oceanic Opt. **6**, 821–826 (1993).
46. V. A. Markel and V. M. Shalaev, "Computational approaches in optics of fractal clusters," in *Computational Studies of New Materials*, D. A. Jelski and T. F. George, eds. (World Scientific, Singapore, 1999), pp. 210–243.
47. D. W. Mackowski, "Electrostatic analysis of radiative absorption by sphere clusters in the Rayleigh limit: application to soot particles," Appl. Opt. **34**, 3535–3545 (1995).
48. D. W. Mackowski and M. Mischenko, "Calculation of the T matrix and the scattering matrix for ensembles of spheres," J. Opt. Soc. Am. A **13**, 2266–2278 (1996).
49. P. B. Johnson and R. W. Christy, "Optical constants of the noble metals," Phys. Rev. B **6**, 4370–4379 (1972).